Absolute electron detachment cross sections of atomic anions of the second and third periods incident on noble gases

F. Zappa, Ginette Jalbert, L. F. S. Coelho, A. B. Rocha, S. D. Magalhães, and N. V. de Castro Faria
Instituto de Física, Universidade Federal do Rio de Janeiro, Caixa Postal 68528, Rio de Janeiro, 21941-972 Rio de Janeiro, Brazil
(Received 13 June 2003; published 13 January 2004)

Anions of the second and third periods—B^-, O^-, F^-, Al^-, S^-, and Cl^-—had their total electron detachment cross sections measured, in the 0.3–1.5 a.u. velocity range, for He, Ne, and Ar targets. It is observed that, for any given target, the cross sections present similar velocity dependence and a conspicuous maximum at the same velocity, which differs for distinct targets. It was also obtained that these cross sections scale with target-independent factors, and the ratio of factors within the same group of the periodic table is also nearly group independent. Explanations for these behaviors are presented considering the presence of low- and high-velocity regions, and describing the latter by a free-electron model. The roles of the double ionization and the strong electron correlation in the detachment process are also discussed.

DOI: 10.1103/PhysRevA.69.012703 PACS number(s): 34.50.Fa, 34.90.+q

I. INTRODUCTION

Negative ions are relevant for a wide range of areas in natural sciences and in technology. In reality, as most of the atoms and molecules possess stable negative ions, these ions are relevant to practically any basic or applied research involving atomic collisions. Among many examples there are the problems of deposition of energy in biological tissue by ionizing radiations, the opacity of stellar atmospheres, the electric discharges in gases and breakdown phenomena, the chemical composition of the upper atmosphere, and the technology of ion sources for tandem accelerators [1–3]. The fact that these negative ions can be accelerated by electric fields, deflected by electric and magnetic fields, and that their outermost electrons are very weakly bound and easily detachable, makes them suitable for applications where a fast neutral beam is required. That is, for example, the case of the diagnosis and heating of fusion plasmas.

Furthermore, negative ions possess dissimilar properties from the corresponding neutral and positive species [1–4], such as the existence of usually only one bound state [4], and the major relevance of electron-electron correlations for their structure and photodetachment [5]. Concerning collisions, the dynamics of electron attachment or detachment collisions has also the peculiarity of a non-Coulombic behavior of the interaction [2].

The theoretical study of anion-atom or anion-molecule collision processes has been done mostly at low energies, with emphasis being placed on the threshold region [6]. At the other extreme, high-velocity collisions of H^- are well described by the Born-approximation including a simplified version called free-collision (or free-electron) model [7]. The intermediate-velocity region, where the velocity of the projectile and of the anion's least-bound-electron are of the same order of magnitude, is not well described by any theoretically sound model.

The experimental study of collisions of intermediate-velocity anions with atoms and molecules has been limited by the lack of appropriate apparatuses. Single-ended accelerators with negative-ion sources placed at a negative high-voltage terminal (of hundred kilovolt, or megavolt) are rare, or nonexistent. Recently we have developed a simple method of measuring absolute cross sections of total electron detachment, in collisions of fast negative atomic or molecular ions, with atoms or molecules, at intermediate velocities [8,9]. It requires a negative-ion source and a tandem accelerator with a gas stripper. The method relies on the electron detachment process that the negative ions undergo in the stripper, placed at the tandem accelerator's high-voltage terminal, which plays the role of a gaseous target. The large range of available collision velocities; the fact that, whatever the values of these velocities, the negative ions leave the accelerator with their (small and constant) initial injection energies; and last, but not least, the fairly stable beam current, which may be assumed constant for time intervals of some minutes, make the method practical and powerful.

The first systematic study that we have done with our method was on the collision of np^3 atomic anions (C^-, Si^-, and Ge^-) with He, Ne, and Ar targets [9], which yielded very interesting results. For each target, the measured cross sections as a function of velocity, for all three anions, arrange themselves along curves of almost the same shape. If for one target these curves are made to coincide with each other, using suitable scale factors, it is found that these factors are the same for the other two targets, i.e., they depend only on the projectile, not on the target. Furthermore, these curves, for a given target, present conspicuous maxima at almost the same velocity. These velocities show a nonmonotonic dependence on the target atomic number.

Considering all these facts, in this paper we make an extensive study of detachment cross sections of anions of the second and third rows of the periodic table of the elements, comparing also with our previous results. The projectiles under study had several configurations: np^2 (B^- and Al^-), np^5 (O^- and S^-), and np^6 (F^- and Cl^-). We analyze these results together with our previous results for np^3 anions (C^-,Si^-), where target-independent scaling rules were obtained. We also measured Na^- detachment, and compared with previous results by Andersen *et al.* for alkali-metal anions (Li^-,Na^-) [10].

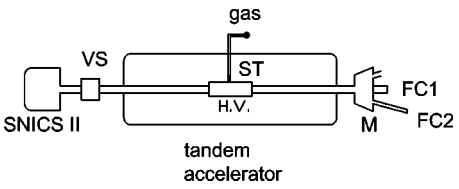

FIG. 1. Experimental setup. SNICS II: sputtering ion source; VS: velocity selector; ST: stripper gas cell; M: magnet; FC1 and FC2: Faraday cups.

II. EXPERIMENT

The experimental setup, located at our institution, is shown in Fig. 1. Only a brief description will be given here of this setup and of the method employed, as they are already described elsewhere [8,9]. Beams of all the studied elements were produced in an ion source (SNICS II) by cesium sputtering using suitable cathodes. The cathodes were obtained by several techniques, most commonly by compressing a mixture of a powdered compound of the element of interest and tungsten powder into an opening in a standard copper support. With these cathodes, currents of microamperes could be extracted. After extraction, the anions were preaccelerated to a kinetic energy T. After mass selection in a Wien filter, they acquired an additional energy eV_0 in the first stage of the tandem accelerator (NEC 5SDH), which ended at the stripper, where V_0, the terminal potential, may be as high as 1.7 MV.

The stripper, considered as a differentially pumped gas cell, consists of a pressurized target chamber placed between the two stages and pumped by two 500-liter/sec turbomolecular pumps at each grounded end of the accelerator tubes. The pressure inside the tubes, with no gas in the cell, is around 10^{-8} torr. This gas cell is 1 cm wide and 47 cm long. In ordinary operation an external container feeds the cell with N_2. The gas pressure inside the cell can be regulated by the opening or closing of an internal admission valve, externally controlled. During the experiments, this pressure was in the 10^{-4} torr range.

The easily replaceable external container led to the possibility of studying different gases. As the gas flow inside the accelerator tube is in the molecular regime, the gas pressure inside the stripper can be derived from measurements of the pressure at the high-energy end of the tube [8,9]. Figure 2 shows one example of the measured H fraction in arbitrary units as a function of the pressure readings (experimental points). We detect the neutral hydrogen atoms through the charge of the secondary electrons that leave a Faraday cup with no electron suppressor. This curve has one free normalization parameter for each axis, as the neutral fraction and the pressure, both measured at the accelerator end, are, respectively, proportional to the neutral fraction at the target exit and to the target pressure. This latter neutral fraction is described by an analytical curve—the solution of the differential equation system describing the charge changing collisions as function of the target pressure—which only depends on well-known experimental cross section values for hydrogen [11,12]. This analytical curve was scaled to the experimental one, the results being displayed in Fig. 2. From this

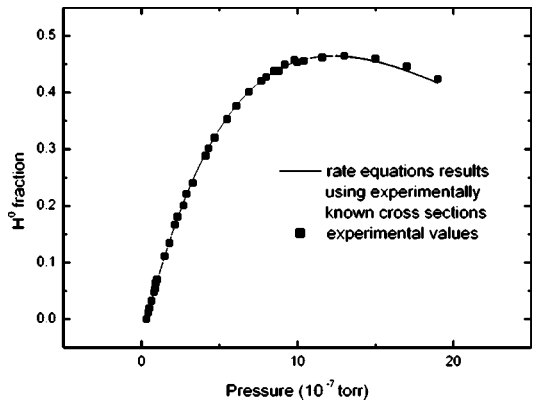

FIG. 2. Measured neutral hydrogen beam fractions vs high energy end pressure (the full line is the analytical curve for neutral fraction as a function of the target pressure, normalized to the measured points).

scaling one obtains the target pressure as a function of the measured high energy end pressure (Fig. 3), the two being proportional in the range 10^{-8}–10^{-6} Torr, as expected for a molecular flow.

The normalization of the incident beam intensity is simplified due to the good stability of the accelerator. In fact, the beam current is constant for time intervals of minutes. The transmitted anions were magnetically deflected, and detected by a Faraday cup. Data acquisition was performed by means of a digital oscilloscope, with output to a personal computer, so the pressure at the high-energy end of the accelerator and the ion current at the Faraday cup at 15° or 0° (Fig. 4) could be recorded simultaneously. The total (and absolute) detachment cross sections were extracted from exponential current decay curves, obtained by varying the target pressure. Uncertainties in the exponential fitting procedure and in the cross section values used in the stripper pressure calibration are the

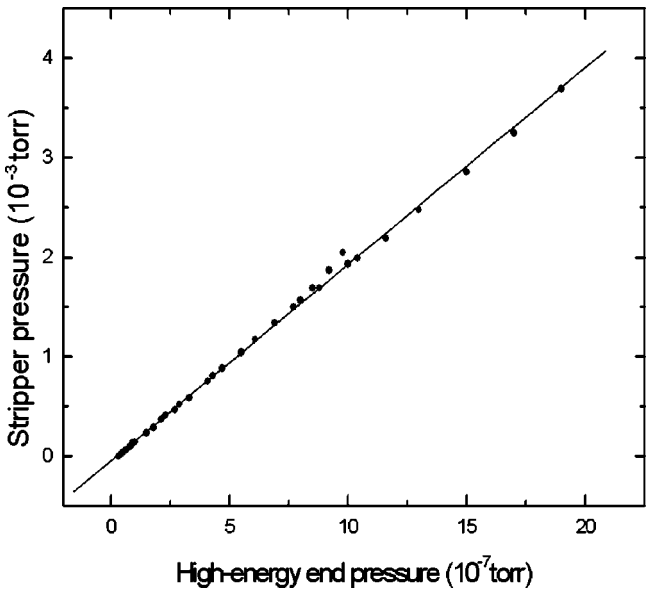

FIG. 3. Calculated stripper pressure vs measured high-energy end pressure.

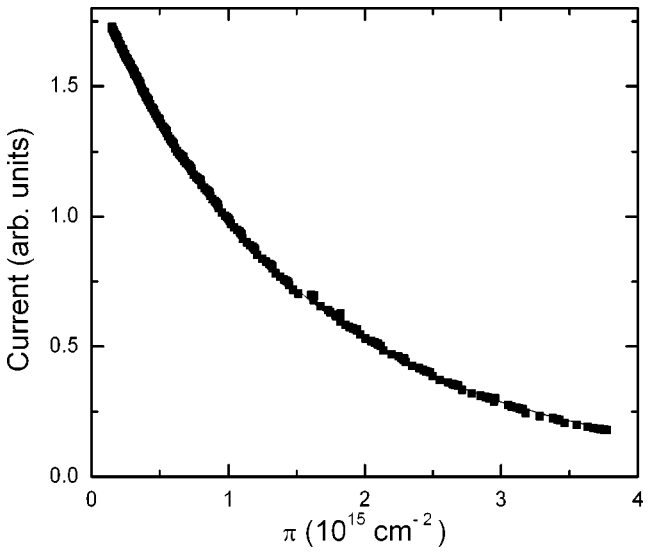

FIG. 4. Typical experimental decay curve used in the measurement of total electron detachment cross sections. It is obtained by varying the target thickness and measuring the final anion current in a Faraday cup (FC2 in Fig. 1).

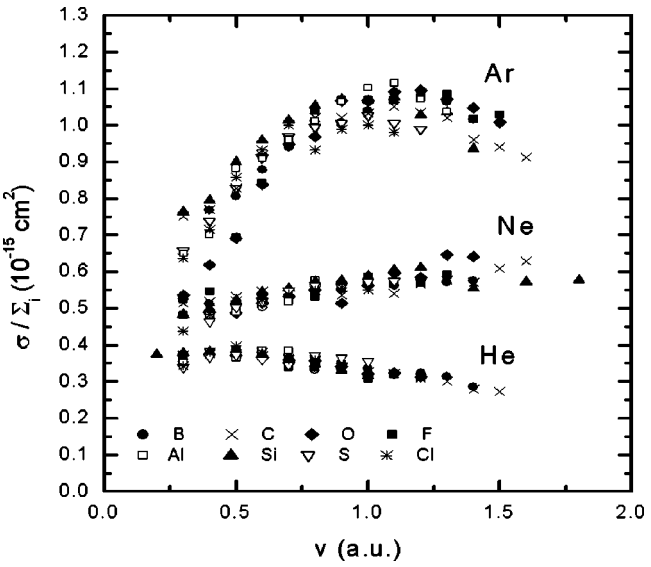

FIG. 5. Total electron detachment cross section for the several np^m anions normalized to the F values incident on He, Ne, and Ar targets, as functions of the relative velocity in atomic units.

main causes of uncertainty in the measured cross sections, estimated to be less than 10%.

III. EXPERIMENTAL RESULTS AND DISCUSSION

The presently measured absolute cross sections, for six np^m anionic projectiles ($n=2,3$; $m=2,5,6$) colliding with three noble gas targets (He, Ne, and Ar), are shown in Table I.

In order to interpret these data one must first point that, as far as the authors are aware, there are neither previous measurements nor calculations for these anionic destruction processes at intermediate velocities.

The second relevant point is that by performing our extensive measurements we were able to verify the presence of several unexpected trends. The following analysis and discussion of the data will be mostly concerned with understanding these seemingly general features.

A. Empirical scalings and curves

The first general trend is that, for any given target, the cross section vs velocity curves for distinct projectiles differ essentially by multiplicative scaling factors. This can be seen in Fig. 5, which presents cross-section values normalized to the F^- cross section (the smallest ones), leading to purely target-dependent curves. A least-square fit procedure was employed to obtain these curves, with the normalization constants Σ being shown in Table II.

This is a surprising phenomena considering the wide choice of anions which, as Table II also shows, have several

TABLE I. Cross sections.

	$\sigma_d(10^{-15}$ cm$^2)$																		
	B			Al			O			S			F			Cl			
v (a.u.)	He	Ne	Ar	He	Ne	Ar	He	Ne	Ar	He	Ne	Ar	He	Ne	Ar	He	Ne	Ar	
0.3				0.730	0.974	1.42			0.625	0.641		1.23	0.370		0.523	0.548	0.677	1.03	
0.4	0.566	0.732	1.15	0.790	0.976	1.53		0.539	0.722	0.694	0.787	1.38	0.380	0.487	0.546	0.605	0.748	1.15	
0.5	0.574	0.737	1.21	0.760	0.990	1.93	0.441	0.536	0.807	0.705	0.854	1.55	0.385	0.507	0.693	0.634	0.805	1.38	
0.6	0.563	0.769	1.32	0.800	1.04	1.99	0.435	0.566	0.978	0.680	0.884	1.71	0.379	0.520	0.841	0.607	0.811	1.50	
0.7	0.531	0.763	1.41	0.800	1.05	2.10	0.428	0.586	1.11	0.654	0.931	1.81	0.340	0.530	0.955	0.574	0.833	1.61	
0.8	0.520	0.781	1.52		1.17	2.22	0.426	0.606	1.13	0.701	0.958	1.86	0.350	0.531	1.04	0.574	0.849	1.50	
0.9	0.510	0.788	1.51			2.33	0.405	0.565	1.24	0.689	0.950	1.88	0.346	0.558	1.07	0.543	0.864	1.59	
1.0	0.505	0.806	1.56			2.42	0.381	0.619	1.24	0.672	0.972	1.92	0.306	0.586	1.07		0.851	1.61	
1.1	0.480	0.803	1.63			2.44	0.385	0.655	1.27		0.977	1.88	0.320	0.567	1.07			1.58	
1.2	0.500	0.824	1.64			2.35	0.372	0.643	1.28			1.85	0.31	0.569	1.07				
1.3	0.490	0.816	1.60			2.27		0.710	1.25					0.592	1.09				
1.4	0.460	0.822	1.52					0.706	1.22						1.02				
1.5			1.51						1.18						1.03				

TABLE II. Cross-section normalization constants Σ, relative to F^-. Previous data from * [8] and ** [10], electron affinities (EA) (eV) [4], and ionization energies I (eV).

	Anion	He	Ne	Ar	EA (eV)	I (eV)
ns^2	Na^-**	2.82	1.89	3.10	0.548	5.14
	Li^-	2.20	1.47	2.41	0.618	5.36
np^2	Al^-	2.08	2.02	2.19	0.441	5.96
	B^-	1.53	1.43	1.50	0.277	8.26
np^3	Si^-*	2.06	1.80	2.02	1.385	8.12
	C^-*	1.61	1.40	1.69	1.263	11.22
np^5	S^-	1.89	1.70	1.87	2.077	10.3
	O^-	1.19	1.10	1.17	1.461	13.55
np^6	Cl^-	1.60	1.55	1.61	3.613	12.95
	F^-	1.00	1.00	1.00	3.401	17.34

configurations and present a large spread both in their electron affinities (EA) and in the ionization energies of their parent atoms (I). This is even more striking as these curves are identical to the ones already measured [8–10] for np^3 ($n=2$–4)—C^-, Si^-, and Ge^-—and ns^2 anions ($n=1$–4)—H^-, Li^-, Na^-, and K^-. Table II includes data for all these anions except for H^-, while Fig. 5, besides the present results, only includes our previous np^3 ($n=2,3$) data, C^- and Si^-, for the sake of clarity.

A detailed examination of Table II reveals some interesting results. First, for any given np^m projectile the He and the Ar normalization factors are almost identical. Second, for all np^m anions the Ne normalization factors, though lying slightly below the other two, still agree with them considering the expected 5% error for each cross-section ratio. This statement is true also for our previously measured C^- and Si^- results [8], showing that the cross sections for all np^m anions can be described as the product of a target-dependent curve by a projectile-dependent normalization factor. A somewhat distinct picture is presented by the alkali anions: He and Ar data are again almost identical but Ne data lie nearly 30% below. Even so one can still speak of roughly target-independent normalization constants for alkali anions [10].

A third result from Table II is that, although the normalization factors Σ only depend on the projectile, they do not present a clear dependence on the projectile electron affinity. For instance, for any given np^m ($n=2,3$) configuration the cross section increases as EA increases, meaning that it would be easier to remove one electron when it is more strongly bound. This is contrary to the observed for alkali-metal anions, when the classically expected inverse square dependence on EA was observed [10]. Reasons for the electron affinity being the relevant parameter for describing the ns^2 but not the np^m anionic destruction are unclear, but they point to distinct mechanisms being at work. Finally, for any given np^m ($n=2,3$) configuration the cross sections decrease as the ionization energy increases.

These two last features could easily be understood if the electron detachment processes were totally dominated by the double electron loss. We rule out this possibility, however, on

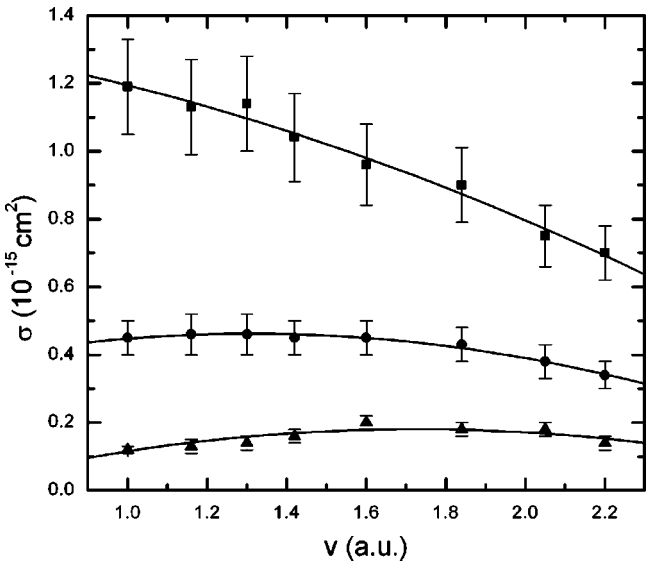

FIG. 6. Detachment cross sections of one (solid square), two (solid circle), and three (solid triangle) electrons of C^- in collision with Ar [9]. The lines are only to guide the eyes.

the following basis: in a recent work [8] we made a study of the relative contribution of the several electron detachment channels in a particular case, measuring single, double, and triple electron-loss cross sections for C^- ions, with velocities between 1.0 and 2.2 a.u., colliding with argon (Fig. 6). The experimental technique employed in that work facilitated measurements at velocities larger than the ones of the present work (0.3–1.5 a.u.) but even so there is a clear feature: as the velocity decreases the single electron loss rises from 60% to 70% of the total cross section, with an upwardard trend for this channel and downward trends for the other two. Consequently single electron loss will be the most influential process for the overall shape of the cross-section curves, though one cannot rule out contributions from the other channels.

The lack of the expected electron affinity dependence together with the presence of an unexpected ionization energy dependence prompted us to look into the $\sigma(3p^m)/\sigma(2p^m)$ ($m=2,3,5,6$) and the $\sigma(3s^2)/\sigma(2s^2)$ ratios. These ratios, defined as the parameters k obtained by dividing the respective normalization factors, are displayed in Table III. They are target independent (within 1%) for any given configuration,

TABLE III. Cross-section ratios for each column of the periodic table, defined as the quotient of the scaling factors Σ of the anions of the third row by the corresponding ones of the second row. The scaling factors came from the normalization procedure illustrated by Fig. 5.

		k			
Structures	Cross-section ratios	He	Ne	Ar	$\langle k \rangle$
ns^2	Σ_{Na}/Σ_{Li}	1.28	1.28	1.28	1.28
np^2	Σ_{Al}/Σ_{B}	1.36	1.41	1.46	1.41
np^3	Σ_{Si}/Σ_{C}	1.28	1.28	1.30	1.29
np^5	Σ_{S}/Σ_{O}	1.59	1.55	1.60	1.58
np^6	σ_{Cl}/Σ_{F}	1.60	1.55	1.61	1.59

and even the smaller values for the Ne normalization factors, evidenced in the previous table, do not affect this almost perfect target independence. Moreover, the average of the ratios for all five configurations yields 1.47 ± 0.14, an uncertainty only slightly exceeding the one for each individual ratio, which is estimated as 7%.

The above discussed trends, presented in Fig. 5, and Tables II and III, do not preclude the existence of small differences, both for the curve shapes and the scaling factors. These differences do exist and can only possibly be explained in a case-by-case study, i.e., one particular anion colliding with a particular target. But it is also clear that the essence of the phenomena is in the explanation of the overall curve similarities, which lead to target-dependent maxima positions, and the several empirical laws, above discussed, governing the scaling parameters.

Concerning the maxima position it is particularly puzzling their lack of display of any anionic dependence, but only a target-dependence. Besides this, as these maxima present a nonmonotonic dependence on the target atomic number, no simple scaling is available for placing together the data for all three noble gas targets into a single universal curve.

B. A two-velocity-regions model

The presence of the maxima in the cross-section curves leads us to define two different velocity regimes. We will consider here that the high velocity region is such where experimental points are at velocities above that where the maximum occurs, and the low velocity is below it. In fact, we assume that the maximum is a region which reflects a smooth change of regime—the relative velocity being high enough to make difficult a quasimolecular approach but not so high as to permit a Born-approximation description.

1. High-velocity region

As a consequence of the above definition, the analysis of this section cannot be employed for Ne targets, because our measurements were taken for velocities below the maximum. Neither can it be employed for Ar targets, due to the small number of high-velocity points. As to He, most points are in the region of interest, except for Al^- and S^-.

Detachment processes at very high velocities are generally well described by the Born approximation, while at not so large velocities the so-called free-collision model (FCM) (also called free-electron model) yields a better agreement with the experimental data [7,15]. In this model it is assumed that the loss of one electron of the projectile is the outcome of a direct interaction of this electron with the target. The electron in the anion is treated as free, and with a velocity that is equal to the velocity of the anion plus the velocity of the electron around the neutral atom. The electron is assumed to be scattered by the target atom with a cross section of the same magnitude as that of a free electron, detachment occurring when the amount of energy transferred to this free electron during the collision surpasses the anion's electron affinity.

A FCM analytical model was developed for electron-loss processes of fast negative and neutral hydrogen projectiles interacting with noble gas targets [16], with a simplified version having already been verified to provide a good description of molecular fragmentation collisions in this velocity region [17].

Two facts suggested that in spite of the excessive simplifications and perhaps naive assumptions of this FCM version it was appropriate to describe the present data. First one had the existence of scaling laws and the decomposition of the cross section into a product of factors depending either on projectile or on the target, a factorization allowed by this FCM simplified version. Also relevant was that the present He target cross-section data, for six anionic projectiles under study, had a velocity dependence similar to the one predicted by that model.

In short, the analytical model of Ref. [16] leads to (with all quantities in atomic units)

$$\sigma = \frac{\sigma_0}{1+(2vR)^2}\frac{\Phi_1}{\Phi_2} Q Z^{C_Q}, \tag{1}$$

where v is the relative velocity and Q and C_Q are target-dependent parameters. R is a scaling radius, empirically found to be smaller than the Thomas-Fermi radius of the target. The other parameters have the following forms:

$$\sigma_0 = 16 Z^2 R^4, \tag{2}$$

$$\Phi_1 = 1 - (v_i/2v)^2, \tag{3}$$

$$\Phi_2 = 1 + (v_i R)^2, \tag{4}$$

$$v_i = (2E_0/m)^{1/2}, \tag{5}$$

with m and E_0 being the mass of the electron and the minimum excitation energy of the projectiles, respectively.

This model was further simplified in Ref. [17]. From the expressions (3) and (4), and taking into account that in the free-collision model regime $v_i \ll v$ and $v_i R$ is small because R is smaller than one, we will consider that the parameters Φ_1 and Φ_2 are close to unity. In that approximation, we can write the very simple velocity dependence:

$$1/\sigma = a + b v^2. \tag{6}$$

In that case, the scaling radius R and the cross section σ may be written as

$$R = \frac{1}{2}\left(\frac{b}{a}\right)^{1/2}, \tag{7}$$

and

$$\sigma = \frac{1/a}{1+(2vR)^2}. \tag{8}$$

When the inverse of the cross sections extracted from Table I (He targets) is plotted as a function of the square of the velocity we get the straight line dependence predicted by Eq.

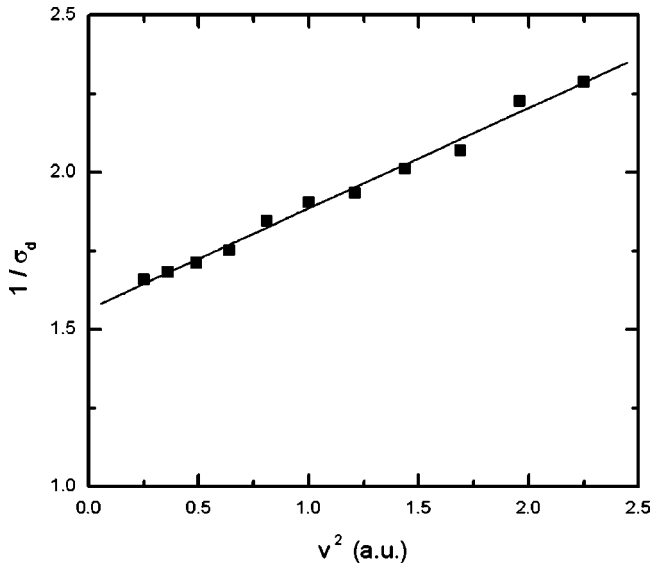

FIG. 7. Example of the linear relationship between $1/\sigma$ and v^2.

(6). Figure 7 shows typical experimental data, carbon inciding upon a helium target with velocities in the 0.5–1.5 a.u. range, fitted to a straight line.

In Table IV we show the scaling radius R, the a and the b parameters, obtained from fitting the experimental data to expression (6). We have always excluded the lower-velocity points, because they are too near the maximum. All R values agree to each other within the experimental uncertainties, providing that R is essentially target dependent as assumed in the model.

The good quality of the fittings using expression (6) indicates that the dependence on the relative velocity of this expression is essentially correct for high velocities. Consequently, in view of Eq. (8), one expects that the normalization factors of Table II should be proportional $(1/a)$. In order to prove that, we divide the scaling factors Σ of Table II by $(1/a)$ entries in Table IV, the results being presented in the last column of Table IV. There we can observe that the obtained values oscillate about their average of 2.44 with an uncertainty of 0.10 (only 4%). The unexpected feature is the almost constancy of the Σ values in Table II for the other targets, since these factors were obtained in different velocity regimes, where expression (6) does not hold. Furthermore, the target independence of the ratios k of the scaling factors Σ, for anions belonging to the same column and distinct rows of the periodic table, colliding with the same target, is just an evidence of the parameter a assuming target-independent and anion-dependent values. Said in another way, it is an evidence of the empirically found factorization of the cross sections into a target and a projectile factors, where the functional behavior with velocity is mainly determined by the target. Published results [18] show that this expression is still valid for molecular targets.

TABLE IV. Fitted parameters a and b [Eq. (6)] and of the scaling radius R for collisions of anions with a He target. The last two columns show Σ (Table II) and the quotient $\Sigma/(1/a)=\Sigma a$.

	a	b	R	Σ	$\Sigma/(1/a)$
B	1.50	0.34	0.24	1.53	2.30
C	1.56	0.32	0.23	1.61	2.51
O	2.16	0.38	0.21	1.19	2.57
F	2.53	0.53	0.23	1.00	2.53
Si	1.16	0.37	0.28	2.06	2.39
Cl	1.48	0.44	0.27	1.60	2.37

The geometric interpretation above, where it is assumed that the loss of one electron of the projectile is due to a direct interaction of this electron with the target, once more points to the simplicity of the collisions of anions in the high-velocity regime. However it is peculiar that in such a simple model the cross sections do not show any simple dependence on the electron affinities, rather appearing more regular with respect to ionization energies. One could guess that the correct parameter should be some combination of the two, as the anions have a strong electron correlation. In view of that it is interesting to notice that there is such quantity, it is called electronegativity, and was qualitatively proposed by Pauling as the ''electron attracting power'' of an atom, and subsequently defined by Mulliken [13] as $\chi=(N_{EA}+I)/2$. Parr *et al.* [14] have proposed a more formal definition of electronegativity, based on the density-functional theory, and have shown that the chemical potential μ for a system, which should measure the easiness for removing one electron, is equal to $-\chi=-(I+N_{EA})/2$.

2. Low-velocity region

One important fact related to the low-velocity regime is its possible influence in the position of the maxima, because the detachment cross sections are very small near the origin and increase with the velocity. In fact, its derivative near the threshold has large influence in the maximum position. At low velocities the quasimolecular approach could, in principle, be used. Accordingly, we have performed *ab initio* potential curve calculations involving the anions and noble gas targets on one hand, and the corresponding neutral atoms and noble gases on the other. This was done in order to verify possible crossings among the two types of potential curves, as suggested by Olson and Liu [19]. This is illustrated in Fig. 8 for carbon anion incident on helium. The detailed description of the calculations will be the object of a separate paper. The Moller-Plesset method up to second order (MP2) was used with a Gaussian $6-311++G(3df,3pd)$ basis set.

These calculations show that, for all studied cases, the curves cross at internuclear distances of about 2 Å for all targets. Even in the cases where the crossing is not present, the curves get closer about this point. According to this model, the probability for detachment has a maximum at the crossing point. In view of that, the closer the atoms could reach, the more effective is the detachment. One expects that helium can penetrate deeper in the electronic cloud of any particular anion when compared with other noble gases, since in its case the number of electrons, and consequently the interelectronic repulsion, is smaller. This explains the enhancement of the cross section for helium at this regime. As

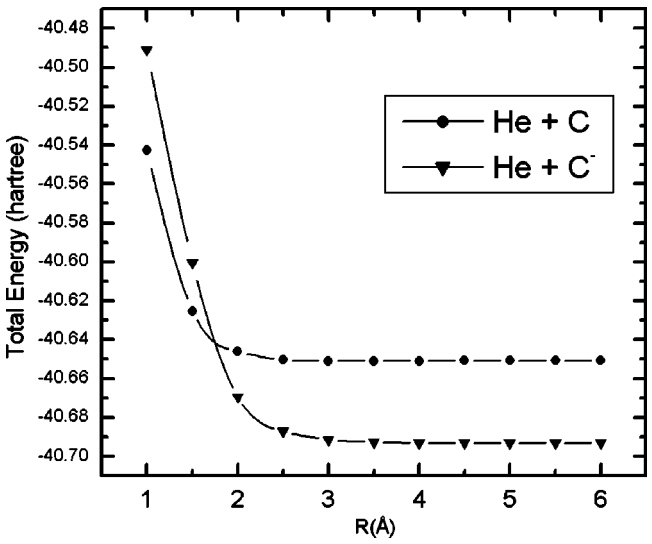

FIG. 8. *Ab initio* potential curves calculation: C and C^- incident on He.

a consequence, the inhibition of the electron detachment by neon with respect to helium makes its smaller cross-section derivative with respect to the velocities, near the threshold, to push the maxima farther from the origin.

IV. CONCLUSIONS

Systematical cross-section data for the total electron detachment of np^m anions of the second and third periods colliding with helium, neon, and argon targets were obtained in the velocity range of 0.1–1.6 a.u. It was observed that they present similar velocity dependence for any given target, with conspicuous maxima at different positions for each target. It was also observed that the cross sections could be factorized into the product of a target-only-dependent curve and a projectile-only-dependent factor Σ. This factor, though presenting a rough linear dependence on the anionic ionization energy I, did not display any similar dependence on the anionic EA.

In order to interpret these projectile-dependent scaling factors cross-section ratios for the same group of the periodic table (thereby presenting similar electronic structures, either np^m or ns^2) were taken. These factors, k, scale with target-independent factors which, besides presenting a very small variation when comparing the three targets, are also identical within a 10% uncertainty when comparing all configurations. These ratios, for p^m configurations, pointed to a distinct behavior from the one presented by alkali anions, namely, the cross sections of the former increased when the electron affinity increased, while the latter had the predicted opposite behavior, i.e., the cross sections had an inverse square dependence on EA.

The peculiar behavior of the electron detachment cross sections was analyzed by a simplified version of the free-collision model and a two-state quasimolecular model, for the high- and the low-velocity regions, respectively. From the former model we observe that these anions, in spite of their wide variation of electron affinities, have detachment cross sections with the same simple velocity dependence: the inverse of the cross sections vary linearly with the square of the velocities. The analysis also strongly supports the actuality of anionic scaling factors Σ, which are proportional to the inverse of the linear coefficients of this fitting.

Moreover, the low-energy analysis has shown that there is an inhibition of the electron detachment process by neon, when compared with helium, with a corresponding decrease in the derivative with respect to the velocity, near threshold. This effect pushes the maximum of the total detachment cross sections, when neon is the target gas, further from the origin than expected, explaining its nonmonotonic correspondence with the target atomic numbers.

ACKNOWLEDGMENTS

This work was partially supported by the Brazilian agencies CNPq, FUJB, and FAPERJ.

[1] H.S.W. Massey, Rep. Prog. Phys. **12**, 248 (1949); *Negative Ions* (Cambrige University Press, Cambridge, 1976); Adv. At. Mol. Phys. **15**, 1 (1979).
[2] W. Earl, Mc.Daniel, J.B.A. Mitchell, and M. Eugene Rudd, *Negative Ions*, Atomic Collisions: Heavy Particle Collisions (Wiley, New York, 1994).
[3] L.G. Christophorou, *Electron-Molecule Interactions and their Applications* (Academic Press, New York, 1984).
[4] T. Andersen, H.K. Haugen, and H. Hotop, J. Phys. Chem. Ref. Data **28**, 1511 (1999).
[5] V.K. Ivanov, J. Phys. B **32**, R67 (1999).
[6] J.M. Rost, Phys. Rev. Lett. **82**, 1652 (1999); F. Robicheaux, *ibid.* **82**, 707 (1999).
[7] D.P. Dewangan and H.R.J. Walters, J. Phys. B **11**, 3983 (1978).
[8] H. Luna, F. Zappa, M.H.P. Martins, S.D. Magalhães, G. Jalbert, L.F.S. Coelho, and N.V. de Castro Faria, Phys. Rev. A **63**, 052716 (2001).
[9] H. Luna, S.D. Magalhães, J.C. Acquadro, M.H.P. Martins, W.M.S. Santos, G. Jalbert, L.F.S. Coelho, and N.V. de Castro Faria, Phys. Rev. A **63**, 022705 (2001).
[10] N. Andersen, T. Andersen, L. Jepsen, and J. Macek, J. Phys. B **17**, 2281 (1984).
[11] Y. Nakai, T. Shirai, T. Tabata, and R. Ito, At. Data Nucl. Data Tables **37**, 69 (1987).
[12] D.P. Almeida, N.V. de Castro Faria, F.L. Freire, Jr., E.C. Montenegro, and A.G. de Pinho, Phys. Rev. A **36**, 16 (1987).
[13] H.O. Pritchard and H.A. Skinner, Chem. Rev. (Washington, D.C.) **55**, 745 (1955).
[14] R.G. Parr, R.A. Donnely, M. Levy, and W.E. Palke, J. Chem. Phys. **68**, 3801 (1978).
[15] J.S. Risley, *Proceedings of the 11th ICPEAC: Invited Papers*, edited by N. Oda and K. Takayanagi (North-Holland, Amsterdam, 1980), pp. 619–630.

[16] M. Meron and B.M. Johnson, Phys. Rev. A **41**, 1365 (1990).
[17] W. Wolff, L.F.S. Coelho, H.E. Wolf, and N.V. de Castro Faria, Phys. Rev. A **45**, 2978 (1992).
[18] F. Zappa, L.F.S. Coelho, S.D. Magalhães, W.M.S. Santos, A.M. Luiz, M.H.P. Martins, A.L.F. de Barros, J.A.M. Pereira, and N.V. de Castro Faria, Phys. Rev. A **67**, 012702 (2003).
[19] R.E. Olson and B. Liu, Phys. Rev. A **17**, 1568 (1978); **20**, 1344 (1979); **22**, 1389 (1980).